Flexible Solid-State Supercapacitors Based on Carbon Nanoparticles/MnO2 Nanorods Hybrid Structure

ARTICLE *in* ACS NANO · DECEMBER 2011

Impact Factor: 12.88 · DOI: 10.1021/nn2041279 · Source: PubMed

Flexible Solid-State Supercapacitors Based on Carbon Nanoparticles/MnO_2 Nanorods Hybrid Structure

Longyan Yuan,[†] Xi-Hong Lu,[†,‡] Xu Xiao,[†] Teng Zhai,[†,‡] Junjie Dai,[†] Fengchao Zhang,[†] Bin Hu,[†] Xue Wang,[§,⊥] Li Gong,[∥] Jian Chen,[∥] Chenguo Hu,[⊥] Yexiang Tong,[‡] Jun Zhou,[†,*] and Zhong Lin Wang[†,§,*]

[†]Wuhan National Laboratory for Optoelectronics (WNLO), and College of Optoelectronic Science and Engineering, Huazhong University of Science and Technology (HUST), Wuhan, 430074, China, [‡]School of Chemistry and Chemical Engineering, Sun Yat-sen University, Guangzhou, 510275, China, [§]School of Materials Science and Engineering, Georgia Institute of Technology, Atlanta, Georgia 30332-0245, United States, [⊥]Department of Applied Physics, Chongqing University, Chongqing 400044, China, and [∥]Instrumental Analysis & Research Center, Sun Yat-sen University, Guangzhou, 510275, China

ABSTRACT

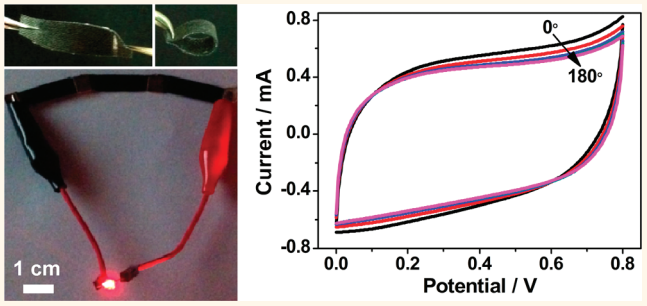

A highly flexible solid-state supercapacitor was fabricated through a simple flame synthesis method and electrochemical deposition process based on a carbon nanoparticles/MnO_2 nanorods hybrid structure using polyvinyl alcohol/H_3PO_4 electrolyte. Carbon fabric is used as a current collector and electrode (mechanical support), leading to a simplified, highly flexible, and lightweight architecture. The device exhibited good electrochemical performance with an energy density of 4.8 Wh/kg at a power density of 14 kW/kg, and a demonstration of a practical device is also presented, highlighting the path for its enormous potential in energy management.

KEYWORDS: flexible · supercapacitors · carbon nanoparticles · MnO_2

Owing to the large proliferation of portable consumer electronics, much effort has been devoted to lightweight, flexible, and even wearable electronics to meet the growing demands of modern society, which is likely to have potential applications including, but not limited to, wearable displays, artificial electronic skin, and distributed sensors.[1−3] All of these electronics require lightweight, flexible, and highly efficient energy management technology. Conventional charge storage devices, such as batteries, have limitations such as short cycle life and relatively slow charging/discharging rates. Electrochemical capacitors (ECs), another state-of-the-art charge storage technique, also known as supercapacitors, have attracted much attention due to their higher power density, longer life cycles than batteries, and higher energy density than dielectric capacitors.[4−6] Much effort has been dedicated to the construction of supercapacitors using carbon-based materials, such as carbon nanotubes (CNTs),[7−12] activated carbon,[13] carbon onions,[14] carbon fibers,[15] and graphene.[16,17] Decorating the surface of carbon materials with pseudocapacitor materials such as RuO_2,[18] NiO,[19] MnO_2,[9,20] and conducting polymers[10,21−23] can further enhance their electrochemical performance.

However, the elaborate procedures to fabricate supercapacitors with CNTs and graphene are complex and expensive to scale up for widespread commercialization.[16,23,24] For safety considerations, a solid-state electrolyte is superior to its liquid counterpart since robust encapsulation is needed to prevent leakage of a liquid electrolyte. In this context, a simplified and low-cost method to fabricate flexible solid-state supercapacitors is greatly desired for portable applications. Here we report a novel and simple method to fabricate solid-state supercapacitors based on a carbon nanoparticles (CNPs)/MnO_2 nanorods hybrid structure using a polyvinyl alcohol (PVA)/H_3PO_4 electrolyte. Carbon fabric is used as a current collector and electrode (mechanical support), leading to a simplified, highly flexible, and lightweight architecture. Also the unique macroporous structure of carbon fabric allows for larger mass loading of the electrolyte. The fabricated supercapacitor exhibits outstanding electrochemical performance, and a demonstration of a practical device is also

* Address correspondence to jun.zhou@mail.hust.edu.cn, zlwang@gatech.edu.

Received for review October 26, 2011 and accepted December 11, 2011.

Published online December 19, 2011
10.1021/nn2041279

presented, highlighting the path for its enormous potential in energy management.

RESULTS AND DISCUSSION

The flexible solid-state supercapacitor was fabricated through a two-step approach. First, CNPs were grown on carbon fabric through a simple and low-cost flame synthesis method.[25,26] The obtained CNPs, with a diameter of about 7 nm, form a nanoporous structure on a carbon fabric substrate.[26] Then MnO_2 nanorods were electrodeposited onto the CNPs.[27] Second, two strips of carbon fabric with a CNPs/MnO_2 nanorods hybrid structure on them were immersed into PVA/H_3PO_4 aqueous solution and solidified together thereafter, with a separator sandwiched between them (experimental details are provided in the Method section). Figure 1a and b show the low- and high-resolution scanning electron microscopy (SEM) images of the carbon fabric after the growth of CNPs and MnO_2 nanorods, respectively. Carbon fabric was woven by carbon fibers with high flexibility and high conductivity. It can be seen that CNPs and MnO_2 grow on carbon fibers axially and uniformly. Figure 1c shows the transmission electron microscopy (TEM) image of the MnO_2 nanorods, revealing that the MnO_2 nanorods have diameters of about 50−100 nm with a length of about 500 nm. The selected area electron diffraction (SAED) pattern (inset of Figure 1c) indicates that the deposited MnO_2 nanorods are crystalline. The hybrid structure was surveyed by X-ray photoelectron spectroscopy (XPS) to verify the chemical composition (Figure S1), and the O 1s and Mn 2p spectra are presented in Figure 1d. The peaks of the O 1s band at 529.7 and 532.0 eV were assigned to Mn−O−Mn and Mn−O−H, respectively, while the two peaks centered at 642.3 and 653.8 eV can be designated to the binding energy of Mn $2p_{3/2}$ and Mn $2p_{1/2}$, respectively, revealing Mn^{4+} ions were dominant in the product.[28]

Cyclic voltammetry (CV) measurements were performed to explore the advantage of bare CNPs and the CNPs/MnO_2 nanorod hybrid structure on carbon fabric as electrochemical electrode using a three-electrode cell in 0.1 M Na_2SO_4 solution. Figure 2a shows the scan rate-dependent CVs for bare CNPs over a range of scan rates of 5−100 mV/s, with a potential window of 0−0.8 V *versus* a saturated calomel electrode (SCE). The areal capacitances of CNPs on carbon fabric were calculated to be 6.1 and 2.4 mF/cm^2 at scan rates of 5 and 100 mV/s, respectively. The current values of CVs for CNPs/15 min MnO_2 electrode were much higher than those of bare CNPs at the same scan rates, and a good symmetrical rectangular shape for CVs at various scan rates can be observed in Figure 2b, showing the capacitive behavior of CNPs can be greatly improved by loading of MnO_2 nanorods. The mass loading was about 0.072, 0.106, 0.201, 0.325, and 0.562 mg for 1, 5, 15, 30, and 45 min MnO_2, respectively. The current increases with the MnO_2 deposition time, which is shown in Figure 2c, leading to the increase of areal capacitance of CNPs/MnO_2 nanorods at various scan rates, which was much higher than that of bare CNPs (Figure S2). The highest areal capacitance of 109 mF/cm^2 was obtained from the electrode at 45 min MnO_2 deposition, approximately 20 times the value for bare CNPs. The present result is much higher than the values reported in the literature (0.4−2 mF/cm^2) for carbon-based supercapacitors.[9,14,29−31]

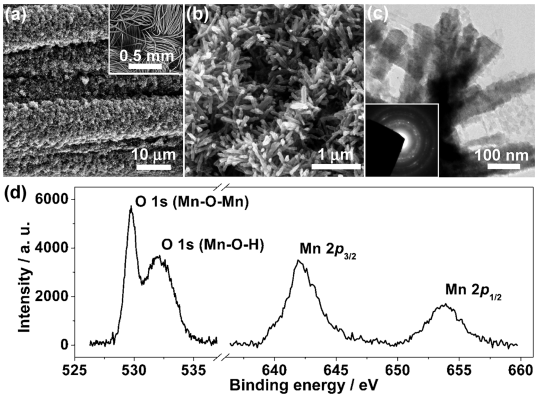

Figure 1. (a, b) SEM images of the CNPs/MnO_2 nanorods hybrid structure on a carbon fabric substrate. The inset in (a) is a low-magnification SEM image of a carbon fabric/CNPs/MnO_2 nanorods hybrid structure. (c) TEM image of a CNPs/MnO_2 nanorods hybrid structure. The inset shows the electron diffraction pattern. (d) XPS survey of O 1s and Mn 2p spectra for MnO_2.

In order to evaluate the contribution of MnO_2 to the electrochemical performance of the CNPs/MnO_2 electrodes, the specific capacitance of MnO_2 was calculated after subtracting the charge of bare CNPs through the equation[32] $C_{s,MnO2} = (Q_{CNPs/MnO2} - Q_{CNPs})/(\Delta V \cdot m_{MnO2})$ and shown in Figure 2d, since the capacitance for bare CNPs was just a small proportion of the hybrid CNPs/MnO_2 electrode. Here $Q_{CNPs/MnO2}$ and Q_{CNPs} are the voltametric charge of the CNPs/MnO_2 and bare CNPs, respectively, and ΔV is 0.8 V. The specific capacitance for 1, 5, 15, 30, and 45 min MnO_2 was about 302, 278, 800, 389, and 165 F/g at a scan rate of 5 mV/s, respectively. The highest specific capacitance was obtained from the 15 min MnO_2, which was higher than that of manganese oxide directly grown on carbon fabric.[33] The specific capacitance for 30 and 45 min MnO_2 was lower than that of 15 min since the increase of mass loading may induce an increase in diameter and length of MnO_2 nanorods, while only a thin layer of MnO_2 was charged and discharged. The CNPs/MnO_2 nanorods hybrid structure not only facilitates the cation diffusion between electrolyte and electrode but also is beneficial to overcome the poor electrical conductivity of MnO_2, both of which would enhance the electrochemical performance of the supercapacitor (Figure S3). A galvanostatic charging/discharging test was conducted in a stable potential

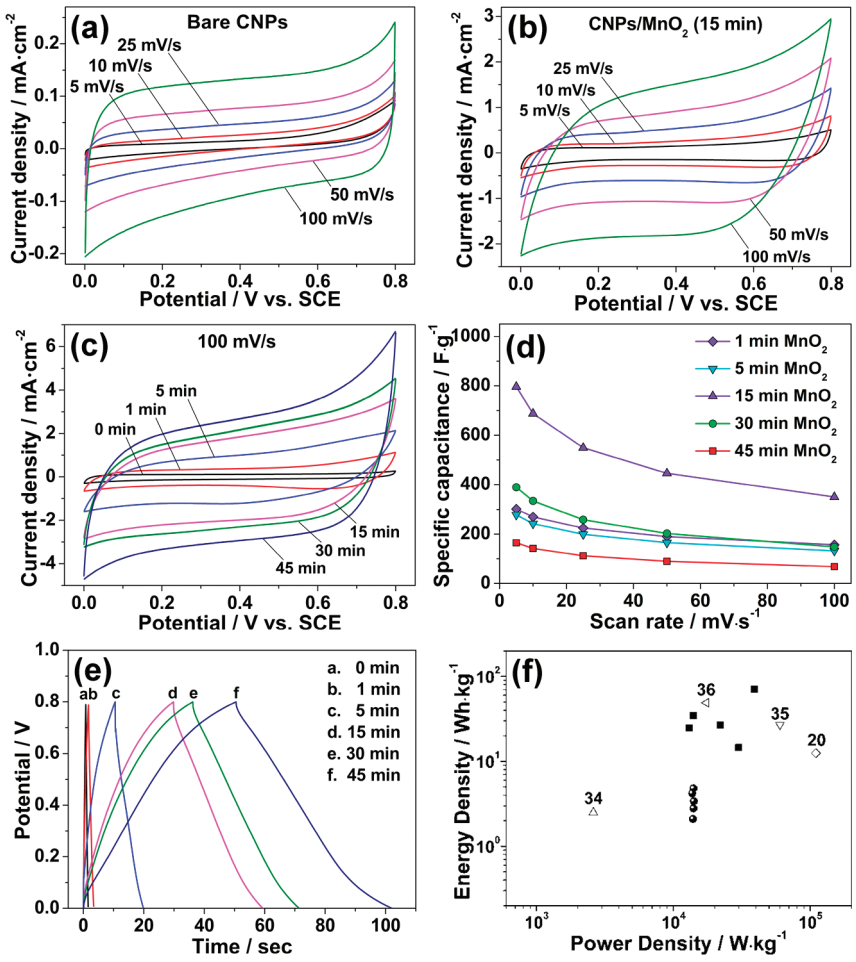

Figure 2. Electrochemical characterization of a CNPs/MnO_2 nanorods hybrid structure on carbon fabric. (a, b) Cyclic voltammetry curves for bare CNPs and CNPs/MnO_2 nanorods (15 min) at different scan rates ranging from 5 to 100 mV/s, respectively. (c) Cyclic voltammetry curves for CNPs/MnO_2 nanorods hybrid structure at a scan rate of 100 mV/s with different MnO_2 deposition time of 0, 1, 5, 15, 30, and 45 min, respectively. (d) Specific capacitance with respect to mass loadings of MnO_2 *versus* scan rates. (e) Galvanostatic charging/discharging curves for CNPs/MnO_2 nanorods hybrid structure at a fixed current density of 1 mA/cm^2. (f) Ragone plot for CNPs/MnO_2 nanorods hybrid structure (solid squares) and solid-state supercapacitor device (solid circles), respectively, compared with the values from refs 20, 34, 35, and 36.

window of 0−0.8 V at a fixed current density of 1 mA/cm^2, and the result is shown in Figure 2e. It reveals that all of the charging curves are symmetrical with their corresponding discharge counterparts, as well as their good linear voltage−time profiles, indicating good capacitive behavior of the hybrid structure. The Ragone plot in Figure 2f shows the high power-energy characteristics of the CNPs/MnO_2 electrodes. The highest power density of 39 kW/kg and the maximum energy density of 71 Wh/kg were achieved, which were comparable to a similar system reported previously using hybrid carbon-based materials/MnO_2 electrodes.[20,34−36]

A solid-state supercapacitor was assembled by two CNPs/MnO_2 nanorod (15 min) hybrid electrodes on carbon fabric. The as-fabricated supercapacitor was lightweight and highly flexible and can be folded and twisted (Figure 3a) without destroying the structural integrity of the device. The CVs in Figure 3b demonstrate that the change of electrochemical performance of the fabricated supercapacitor seems to be subtle and acceptable under different bending angles. In addition, the rectangular profile and symmetry of CVs show the ideal pseudocapacitive nature of MnO_2 and fast redox reaction with PVA/H_3PO_4 solid electrolyte. The galvanostatic charge/discharge result is shown in Figure 3c. Both the linear profile of charge and discharge curves and their symmetry reveal the good capacitive characteristics of the solid-state supercapacitor device. It has an energy density of 4.8 Wh/kg at a power density of 14 kW/kg (Figure 2f). The leakage current of the as-fabricated device was very small, which was about 15 μA after 200 s from the start and then stable at about 10 μA for a long time beyond 2 h (Figure S4). This value is lower than that of the CNT/PANI supercapacitor,[10] demonstrating fewer impurities in the capacitor materials and/or its electrolyte in the fabricated device.[37] The self-discharge of the fabricated solid-state device was also tested, and the result is plotted in Figure S5. The device underwent a

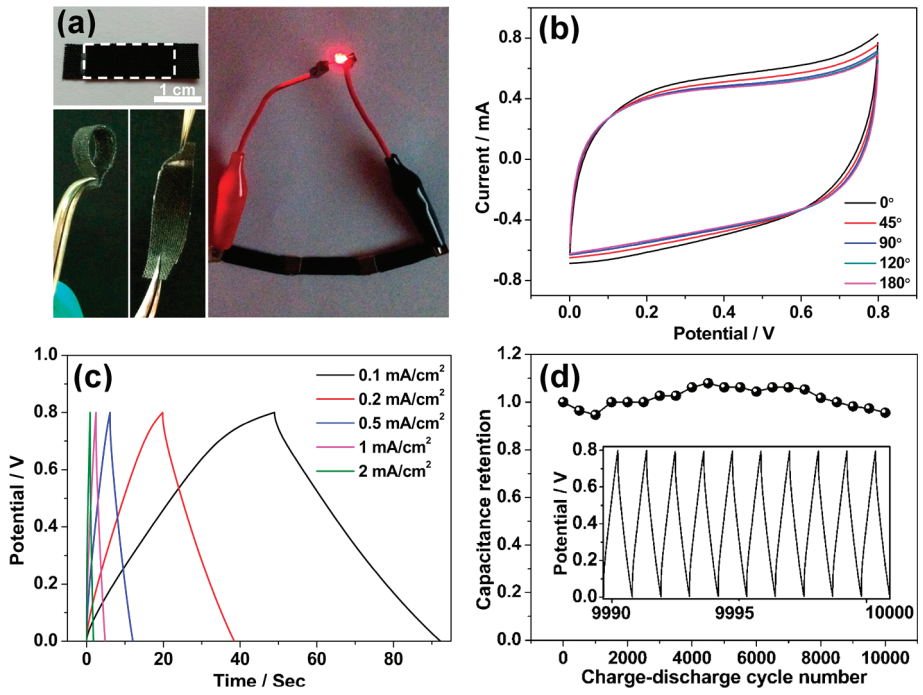

Figure 3. (a) Optical photographs of the fabricated solid-state supercapacitor device. The square indicates the capacitance region. The left bottom images show the flexibility of the device. The right image shows a light-emitting-diode (LED) lighting by a device composed of three supercapacitors connected in series. (b) Cyclic voltammetry curves for a CNPs/MnO_2 nanorod supercapacitor at different curvatures of 0°, 45°, 90°, 120°, and 180°. (c) Galvanostatic charging/discharging curves for CNPs/MnO_2 nanorod solid-state supercapacitor at different current densities. (d) Cycling stability of a CNPs/MnO_2 nanorod supercapacitor device over 10 000 cycles. The inset shows the galvanostatic charge/discharge curve for the device.

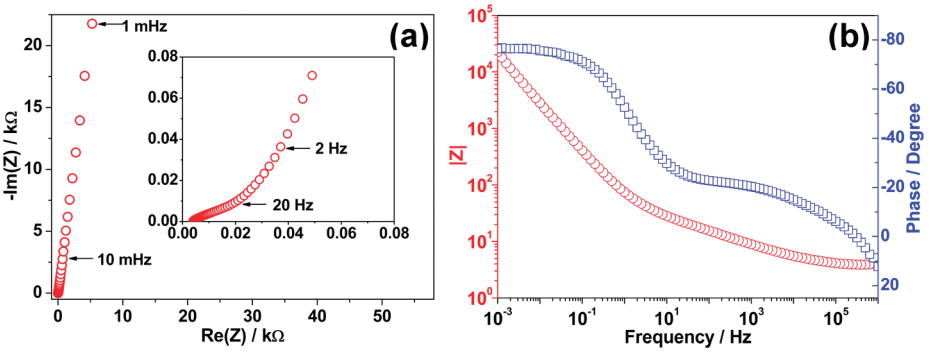

Figure 4. (a) Nyquist and (b) Bode plots of the solid-state supercapacitor device with CNPs/MnO_2 nanorod hybrid structure, respectively.

rapid self-discharge process in the first few minutes, which gradually slowed after several hours. Finally the output voltage of the device reached about 0.2 V after 24 h. The long-term cycling stability of the supercapacitor was tested through a cyclic charge/discharge process at a fixed current density of 1 mA/cm^2, which is shown in Figure 3d. The supercapacitor device still remains at 97.3% of the initial capacitance after 10 000 charge/discharge cycles, demonstrating its excellent long-term cycling stability. The inset reveals no significant electrochemical change during the long-term charging and discharging process after cycling 10 000 times.

An electrochemical impedance spectroscopy (EIS) test was carried out in a frequency range from 1 mHz to 1 MHz to further evaluate the electrochemical behaviors of the fabricated solid-state supercapacitor. As shown in Nyquist plots in Figure 4a, the straight line nearly parallel to the imaginary axis showed the ideal capacitive behavior of the device. The intercept of the Nyquist curve on the real axis is about 4 Ω, manifesting the good conductivity of the electrolyte and very low internal resistance of the electrode. The "knee frequency" of the supercapacitor is about 2 Hz, showing that a pure capacitive behavior can be obtained and most of its stored energy is accessible at frequencies below this frequency.[14,38] Figure 4b displays the Bode plots of the as-fabricated supercapacitor. It can be observed that the capacitor response frequency, f_0, at the phase angle of −45° was about 2 Hz, as expected

(also seen in Figure S6), which is even comparable to the values for supercapacitors with aqueous electrolytes.[39] Thus the relaxation time constant τ_0 was calculated to be about 0.5 s by the equation $\tau_0 = 1/f_0$. The phase angle of the supercapacitor was about −77° at a frequency of 1 mHz, close to −90° for ideal capacitors, coinciding with the RC (a serial resistance R and capacitance C) equivalent circuit for supercapacitors.

Furthermore, we had connected three supercapacitor units in series to light a light-emitting diode (LED). Every device used here has the same area of about 1 cm^2. The whole device showed great electrochemical performance, which was confirmed through CVs and galvanostatic charging/discharging measurements (Figure S7). After charging at 1 mA for 30 s, the device could light the LED for over 20 min, which can be seen in Figure 3a. This result reveals the potential of the fabricated flexible supercapacitor device in energy storage.

CONCLUSION

In summary, a solid-state supercapacitor based on a CNPs/MnO_2 nanorod hybrid structure was fabricated through a simple flame synthesis method and electrochemical deposition process. The device exhibited good electrochemical performance with an energy density of 4.8 Wh/kg at a power density of 14 kW/kg. The demonstration for its practical use indicates the great potential application in energy management for flexible and lightweight electronics.

METHODS

Synthesis. Carbon fabric with a thickness of about 360 μm (weight: 125 g/m^2) was used as the substrate. CNPs were grown on carbon fabric through an ethanol flame synthesis method we reported previously.[26] In short, strips of carbon fabric were located in the flame center for 30 s, then moved away, and CNPs grew on the side facing the ethanol flame. Then anodic electrodeposition of MnO_2 was performed at a constant current of 0.5 mA/cm^2 in a solution of 0.01 M manganese acetate ($MnAc_2$) and 0.02 M ammonium acetate (NH_4Ac) containing 10% dimethyl sulfoxide (DMSO) at 70 °C. Before the electrodeposition process, ethanol or 2-propanol was dropped onto the carbon fabric to make it hydrophilic. The deposition process continued for 1 to 45 min, and then the carbon fabric was taken out and washed with deionized water thoroughly.

Fabrication of Solid-State Supercapacitor. The PVA/H_3PO_4 gel electrolyte was prepared as follows: 6 g of H_3PO_4 was added into 60 mL of deionized water, and then 6 g of PVA power was added. The whole mixture was heated to 85 °C under stirring until the solution became clear. Two strips of the obtained fabric with CNPs/MnO_2 were immersed into the PVA/H_3PO_4 solution for 3 min, keeping the bare carbon fabric part without CNPs above the solution, then taken out and assembled together with a separator (NKK TF40, 40 μm) sandwiched in between, leaving aside the bare carbon fabric part as the electrode. After the PVA/H_3PO_4 gel solidified at room temperature, the solid-state supercapacitor was prepared.

Characterization. The morphologies, chemical composition, and the structure of the products were characterized by high-resolution field emission scanning electron microscopy (FEI Sirion 200), transmission electron microscopy (JEOL 4000EX), and XPS (Thermofisher-ESCALab 250). The cyclic voltammetry and galvanostatic charging/discharging measurements were conducted with an electrochemical station (CHI 660D), and the electrochemical impedance spectroscopy was measured by an Autolab PGSTAT302N at a frequency ranging from 1 mHz to 1 MHz with a potential amplitude of 10 mV. Inductively coupled plasma atomic emission spectroscopy (SPECTRO) was used to analyze the loading of MnO_2. The leakage current was measured through a battery test system (LAND, CT2001A). The self-discharge was tested through a low-noise preamplifier (Standford Research Systems, model SR560).

Acknowledgment. L.Y.Y. and X.H.L. contributed equally to this work. This work was financially supported by the National Natural Science Foundation of China (51002056), Foundation for the Author of National Excellent Doctoral Dissertation of PR China (201035), National Basic Research Program of China (2012CB619302), the Program for New Century Excellent Talents in University (NCET-10-0397), China Postdoctoral Science Foundation (20100480892), and Huazhong University (01-24-182021, 01-24-187051). The authors thank the Analysis and Testing Center of Huazhong University of Science and Technology for support.

Supporting Information Available: TEM image and SAED pattern for CNPs/5 min MnO_2, XPS survey for CNPs/MnO_2 nanorods, areal capacitance for CNPs/MnO_2 nanorod hybrid structure with different MnO_2 deposition times, leakage current and self-discharge of the solid-state supercapacitor, real and imaginary part capacitance *versus* frequency, and cyclic voltammetry and galvanostatic charging/discharging curves for three supercapacitors connected in series. This material is available free of charge *via* the Internet at http://pubs.acs.org.

REFERENCES AND NOTES

1. Rogers, J. A.; Huang, Y. G. A Curvy, Stretchy Future for Electronics. *Proc. Natl. Acad. Sci. U. S. A.* **2009**, *106*, 10875–10876.
2. Kim, D. H.; Lu, N.; Ma, R.; Kim, Y. S.; Kim, R. H.; Wang, S.; Wu, J.; Won, S. M.; Tao, H.; Islam, A.; *et al*. Epidermal Electronics. *Science* **2011**, *333*, 838–843.
3. Someya, T.; Kato, Y.; Sekitani, T.; Iba, S.; Noguchi, Y.; Murase, Y.; Kawaguchi, H.; Sakurai, T. Conformable, Flexible, Large-Area Networks of Pressure and Thermal Sensors with Organic Transistor Active Matrixes. *Proc. Natl. Acad. Sci. U. S. A.* **2005**, *102*, 12321–12325.
4. Conway, B. E. *Electrochemical Supercapacitors: Scientific, Fundamentals and Technological Applications*; Plenum: New York, 1999; pp 19−20.
5. Miller, J. R.; Simon, P. Electrochemical Capacitors for Energy Management. *Science* **2008**, *321*, 651–652.
6. Simon, P.; Gogotsi, Y. Materials for Electrochemical Capacitors. *Nat. Mater.* **2008**, *7*, 845–854.
7. Frackowiak, E.; Béguin, F. Electrochemical Storage of Energy in Carbon Nanotubes and Nanostructured Carbons. *Carbon* **2002**, *40*, 1775–1787.
8. Du, C. S.; Pan, N. Supercapacitors Using Carbon Nanotubes Films by Electrophoretic Deposition. *J. Power Sources* **2006** *160*, 1487–1494.
9. Kaempgen, M.; Chan, C. K.; Ma, J.; Cui, Y.; Gruner, G. Printable Thin Film Supercapacitors Using Single-Walled Carbon Nanotubes. *Nano Lett.* **2009**, *9*, 1872–1876.
10. Meng, C.; Liu, C.; Chen, L.; Hu, C.; Fan, S. Highly Flexible and All-Solid-State Paperlike Polymer Supercapacitors. *Nano Lett.* **2010**, *10*, 4025–4031.
11. Hu, L. B.; Pasta, M.; La Mantia, F.; Cui, L. F.; Jeong, S.; Deshazer, H. D.; Choi, J. W.; Han, S. M.; Cui, Y. Stretchable, Porous, and Conductive Energy Textiles. *Nano Lett.* **2010**, *10*, 708–714.
12. Hu, L. B.; Choi, J. W.; Yang, Y.; Jeong, S.; La Mantia, F.; Cui, L. F.; Cui, Y. Highly Conductive Paper for Energy-Storage

Devices. *Proc. Natl. Acad. Sci. U. S. A.* **2009**, *106*, 21490–21494.
13. Pandolfo, A. G.; Hollenkamp, A. F. Carbon Properties and Their Role in Supercapacitors. *J. Power Sources* **2006**, *157*, 11–27.
14. Pech, D.; Brunet, M.; Durou, H.; Huang, P.; Mochalin, V.; Gogotsi, Y.; Taberna, P. L.; Simon, P. Ultrahigh-Power Micrometre-Sized Supercapacitors Based on Onion-Like Carbon. *Nat. Nanotechnol.* **2010**, *5*, 651–654.
15. Frackowiak, E.; Béguin, F. Carbon Materials for the Electrochemical Storage of Energy in Capacitors. *Carbon* **2001**, *39*, 937–950.
16. Wang, Y.; Shi, Z.; Huang, Y.; Ma, Y.; Wang, C.; Chen, M.; Chen, Y. Supercapacitor Devices Based on Graphene Materials. *J. Phys. Chem. C* **2009**, *113*, 13103–13107.
17. Jeong, H. M.; Lee, J. W.; Shin, W. H.; Choi, Y. J.; Shin, H. J.; Kang, J. K.; Choi, J. W. Nitrogen-Doped Graphene for High-Performance Ultracapacitors and the Importance of Nitrogen-Doped Sites at Basal Planes. *Nano Lett.* **2011**, *11*, 2472–2477.
18. Miller, J. M.; Dunn, B.; Tran, T. D.; Pekala, R. W. Deposition of Ruthenium Nanoparticles on Carbon Aerogels for High Energy Density Supercapacitor Electrodes. *J. Electrochem. Soc.* **1997**, *144*, L309–L311.
19. Yuan, C.; Zhang, X.; Su, L.; Gao, B.; Shen, L. Facile Synthesis and Self-Assembly of Hierarchical Porous NiO Nano/Micro Spherical Superstructures for High Performance Supercapacitors. *J. Mater. Chem.* **2009**, *19*, 5772–5777.
20. Yu, G.; Hu, L.; Vosgueritchian, M.; Wang, H.; Xie, X.; McDonough, J. R.; Cui, X.; Cui, Y.; Bao, Z. Solution-Processed Fraphene/MnO_2 Nanostructured Textiles for High-Performance Electrochemical Capacitors. *Nano Lett.* **2011**, *11*, 2905–2911.
21. Frackowiak, E.; Khomenko, V.; Jurewicz, K.; Lota, K.; Béguin, F. Supercapacitors Based on Conducting Polymers/Nanotubes Composites. *J. Power Sources* **2006**, *153*, 413–418.
22. Zhang, K.; Zhang, L. L.; Zhao, X. S.; Wu, J. Graphene/Polyaniline Nanofiber Composites as Supercapacitor Electrodes. *Chem. Mater.* **2010**, *22*, 1392–1401.
23. Wu, Q.; Xu, Y.; Yao, Z.; Liu, A.; Shi, G. Supercapacitors Based on Flexible Graphene/Polyaniline Nanofiber Composite Films. *ACS Nano* **2010**, *4*, 1963–1970.
24. Wang, D. W.; Li, F.; Zhao, J.; Ren, W.; Chen, Z. G.; Tan, J.; Wu, Z. S.; Gentle, I.; Lu, G. Q.; Cheng, H. M. Fabrication of Graphene/Polyaniline Composite Paper *via in situ* Anodic Electropolymerization for High-Performance Flexible Electrode. *ACS Nano* **2009**, *3*, 1745–1752.
25. Yuan, L. Y.; Dai, J. J.; Fan, X. H.; Song, T.; Tao, Y. T.; Wang, K.; Xu, Z.; Zhang, J.; Bai, X. D.; Lu, P. X.; *et al.* Self-Cleaning Flexible Infrared Nanosensor Based on Carbon Nanoparticles. *ACS Nano* **2011**, *5*, 4007–4013.
26. Yuan, L. Y.; Tao, Y. T.; Chen, J.; Dai, J. J.; Song, T.; Ruan, M. Y.; Ma, Z. W.; Gong, L.; Liu, K.; Zhang, X. H.; *et al.* Carbon Nanoparticles on Carbon Fabric for Flexible and High-Performance Field Emitters. *Adv. Funct. Mater.* **2011**, *21*, 2150–2154.
27. Lu, X.; Zheng, D.; Zhai, T.; Liu, Z.; Huang, Y.; Xie, S.; Tong, Y. Facile Synthesis of Large-Area Manganese Oxide Nanorod Aarrays as a High-Performance Electrochemical Supercapacitor. *Energy Environ. Sci.* **2011**, *4*, 2915–2921.
28. Toupin, M.; Brousse, T.; Bélanger, D. Charge Storage Mechanism of MnO_2 Electrode Used in Aqueous Electrochemical Capacitor. *Chem. Mater.* **2004**, *16*, 3184–3190.
29. Bae, J.; Song, M. K.; Park, Y. J.; Kim, J. M.; Liu, M.; Wang, Z. L. Fiber Supercapacitors Made of Nanowire-Fiber Hybrid Structures for Wearable/Flexible Energy Storage. *Angew. Chem., Int. Ed.* **2011**, *50*, 1683–1687.
30. In, H. J.; Kumar, S.; Shao-Horn, Y.; Barbastathis, G. Origami Fabrication of Nanostructured, Three-Dimensional Devices: Electrochemical Capacitors with Carbon Electrodes. *Appl. Phys. Lett.* **2006**, *88*, 083104.
31. Gao, W.; Singh, N.; Song, L.; Liu, Z.; Reddy, A. L. M.; Ci, L.; Vajtai, R.; Zhang, Q.; Wei, B.; Ajayan, P. M. Direct Laser Writing of Micro-Supercapacitors on Hydrated Graphite Oxide Films. *Nat. Nanotechnol.* **2011**, *6*, 496–500.
32. Lang, X.; Hirata, A.; Fujita, T.; Chen, M. Nanoporous Metal/Oxide Hybrid Electrodes for Electrochemical Supercapacitors. *Nat. Nanotechnol.* **2011**, *6*, 232–236.
33. Wu, M. S.; Guo, Z. S.; Jow, J. J. Highly Regulated Electrodeposition of Needle-Like Manganese Oxide Nanofibers on Carbon Fiber Fabric for Electrochemical Capacitors. *J. Phys. Chem. C* **2010**, *114*, 21861–21867.
34. Wu, Z. S.; Ren, W.; Wang, D. W.; Li, F.; Liu, B.; Cheng, H. M. High-Energy MnO_2 Nanowire/Graphene and Graphene Asymmetric Electrochemical Capacitors. *ACS Nano* **2010**, *4*, 5835–5842.
35. Chen, P. C.; Shen, G.; Shi, Y.; Chen, H.; Zhou, C. Preparation and Characterization of Flexible Asymmetric Supercapacitors Based on Transition-Metal-Oxide Nanowire/Single-Walled Carbon Nanotube Hybrid Thin-Film Electrodes. *ACS Nano* **2010**, *4*, 4403–4411.
36. Kim, J. H.; Lee, K. H.; Overzet, L. J.; Lee, G. S. Synthesis and Electrochemical Properties of Spin-Capable Carbon Nanotube Sheet/MnO_x Composites for High-Performance Energy Storage Devices. *Nano Lett.* **2011**, *11*, 2611–2617.
37. Conway, B. E. *Electrochemical Supercapacitors: Scientific, Fundamentals and Technological Applications*; Plenum: New York, 1999; pp 560−561.
38. Taberna, P. L.; Simon, P.; Fauvarque, J. F. Electrochemical Characteristics and Impedance Spectroscopy Studies of Carbon-Carbon Supercapacitors. *J. Electrochem. Soc.* **2003** *150*, A292–A300.
39. Meng, F.; Ding, Y. Sub-Micrometer-Thick All-Solid-State Supercapacitors with High Power and Energy Densities. *Adv. Mater.* **2011**, *23*, 4098–4102.